Predicting plant immunity gene expression by identifying the decoding mechanism of calcium signatures

Gioia Lenzoni, Junli Liu*, and Marc R. Knight*

Department of Biosciences, Durham University, South Road, Durham DH1 3LE, UK.

*Correspondence: MRK (email: m.r.knight@durham.ac.uk; tel: 0191 334 1224) and JL (email: junli.liu@durham.ac.uk; tel: 0191 334 1376)

Brief heading: Mechanism of decoding calcium signatures

Total word count: 5786

Introduction word count: 800

Materials and Methods word count: 1267

Results word count: 2160

Discussion word count: 1553

Acknowledgements word count: 15

Total number of figures: 6

Number of figures to be published in colour: 5

Supplementary tables: 2

Supplementary figures: 8

Summary

- Calcium plays a key role in determining the specificity of a vast array of signalling pathways in plants. Cellular calcium elevations with different characteristics (calcium signatures) carry information on the identity of the primary stimulus, ensuring appropriate downstream responses. However, the mechanism for decoding calcium signatures is unknown. To determine this, decoding of the SA-mediated plant immunity signalling network controlling gene expression was examined.

- A dynamic mathematical model of the SA-mediated plant immunity network was developed. This model was used to predict responses to different calcium signatures; these were validated empirically using quantitative real-time PCR to measure gene expression.

- The mechanism for decoding calcium signatures to control expression of plant immunity genes *EDS1* and *ICS1* was identified. Calcium, calmodulin, CAMTA3 and CBP60g together amplify each calcium signature into three active signals, simultaneously regulating expression. The time required for calcium to return to steady-state level also quantitatively regulates gene expression.

- Decoding of calcium signatures occurs via nonlinear interactions between these active signals, producing a unique response in each case. Key properties of the calcium signatures are not intuitive, exemplifying the importance of mathematical modelling approaches. This approach can be applied to identifying the decoding mechanisms of other plant calcium signalling pathways.

Keywords

calcium signalling, gene expression, modelling, plant immunity, specificity, decoding, salicylic acid.

Introduction

The second messenger calcium plays a key role in the specificity of signalling pathways in eukaryotes as it controls a vast array of cellular responses (Berridge *et al.*, 2003; Clapham, 2007). Interestingly, different primary stimuli lead to cellular calcium elevations with different kinetics, each distinct calcium elevation being termed a “calcium signature” (McAinsh & Pittman, 2009). Of key importance is that information in the form of calcium signatures is used by cells to specify the nature and severity of the primary simulus (McAinsh & Pittman, 2009; Ranty *et al.*, 2016). Thus, calcium signatures encode specific

information that can be decoded by cells to elicit the appropriate response; *e.g*. recognition of plant pathogenic and symbiotic microbes (Zipfel & Oldroyd, 2017), expression of stress genes in plants (Whalley & Knight, 2013) and closure of guard cells (Allen *et al.*, 2001). Without the correct calcium signature, the plant does not activate the appropriate response to a given stress, and therefore does not adapt to the new condition, affecting its fitness to survive. The specific information carried by calcium signatures is relayed to the end response via calcium-binding proteins: the "decoders" (Hashimoto & Kudla, 2011). In the case of regulation of gene expression specifically, we have previously shown that different calcium signatures can regulate different genes, by controlling different transcription factors (Whalley & Knight, 2013). For one specific case, the calmodulin-binding transcription activators transcription factors (CAMTA), we developed a model to explain the differential activation of these transcription factors in response to different calcium signatures (Liu *et al.*, 2015).

The fundamental question of how specific calcium signatures are decoded to produce the correct appropriate response, however, is not yet known. In this paper we take a combined modelling and experimental approach to answer this question using the expression of genes involved in salicylic acid (SA) regulated plant immunity as an example. It has been demonstrated that increases in calcium, and the calcium binding proteins responding to these increases in calcium, are necessary for plant immunity (Kim *et al.*, 2002; McAinsh & Pittman, 2009; Dodd *et al.*, 2010; Galon *et al.*, 2010; Kudla *et al.*, 2010; Seybold *et al.*, 2014; Tsuda & Somssich, 2015). One of the primary roles of calcium signalling in plant immunity is the regulation of SA biosynthesis (Zhang *et al.*, 2010; Zhang *et al.*, 2014). SA is a phytohormone that plays a central role in plant defence signalling (Vlot *et al.*, 2009), specifically regulating the changes in nuclear gene expression which are required for activating plant resistance. Calcium has been demonstrated empirically to play a very prominent role in controlling the plant immune response (Kim *et al.*, 2009; Seybold *et al.*, 2014) including SA biosynthesis. In particular, different calcium-associated transcription factors, such as CAMTA3 (AtSR1) and CBP60g, regulate gene expression in plant immunity (Zhang *et al.*, 2010; Zhang *et al.*, 2014). CAMTA3 and CBP60g are well characterised Ca^{2+}/calmodulin (CaM)-regulated transcription factors and both have a CaM binding domain (Finkler *et al.*, 2007; Galon *et al.*, 2008; Kim *et al.*, 2009; Wang *et al.*, 2009; Zhang *et al.*, 2010; Reddy *et al.*, 2011; Wang *et al.*, 2011; Bickerton & Pittman, 2012; Poovaiah *et al.*,

2013). Several genes involved in mediating plant immunity are regulated by these transcription factors. For example, *EDS1 (enhanced disease susceptibility 1)*, part of the SA network, was reported to be directly regulated by AtSR1 (CAMTA3) (Du *et al.*, 2009). Expression of *ICS1* (*isochorismate synthase 1*) is similarly regulated by CBP60g (Wang *et al.*, 2009; Zhang *et al.*, 2010; Wang *et al.*, 2011) and *ICS1* encodes a key enzyme in salicylic acid (SA) production (Zhang *et al.*, 2010). Expression of these genes thus plays a key role in plant immunity by regulating the levels of the plant defence hormone salicylic acid (Zhang *et al.*, 2010; Zhang *et al.*, 2014). Therefore, in this way, calcium plays a pivotal role in fine-tuning SA biosynthesis through the simultaneous positive regulation of ICS1 (promoting SA production) and EDS1 (which is a positive regulator of ICS1) during response to pathogens.

Whilst it is known that Ca^{2+} signals are of key importance for the activation of plant immunity (Kim *et al.*, 2002; McAinsh & Pittman, 2009; Dodd *et al.*, 2010; Galon *et al.*, 2010; Kudla *et al.*, 2010; Seybold *et al.*, 2014; Tsuda & Somssich, 2015), and that different calcium signatures are generated in response to different microbial pathogens (Grant *et al.*, 2000), it is not yet known how the signatures are decoded by cells to produce the appropriate specific gene expression pattern essential for immunity. It is to answer this intriguing question that the research presented here is aimed. The mathematical model we developed as a consequence was able to predict patterns of *ICS1* and *EDS1* gene expression in response to different calcium signatures, which were validated empirically. This approach can be applied to identifying the decoding mechanisms of other plant calcium signalling pathways.

Materials and Methods

Plant materials, growth conditions and treatments with calcium agonists. Experiments were performed on transgenic *Arabidopsis thaliana* L. (Heyn) lines constitutively expressing 35S::apoaequorin in the cytosol (pMAQ2, Col-0 ecotype, (Knight *et al.*, 1991)). Seeds were ethanol-sterilised, sown on 1 X Murashige and Skoog (MS, Duchefa Biochemie) medium pH 5.8 (Murashige & Skoog, 1962), 0.8% (w/v) agar (Sigma-Aldrich) on Petri dishes, stratified for a minimum of 48 h at 4^{o}C before growing them at 20^{o}C with a 16/8 h photoperiod at a light intensity of 150 µmol m^{-2} s^{-1}. Calcium measurements and agonist treatments were performed on 8-day-old seedlings; aequorin reconstitution was performed on 7-day-old seedlings. For all the chemical treatments, 7 day-old *Arabidopsis* seedlings were floated in

water in the dark overnight (Knight & Knight, 1995). The next day seedlings were transferred to a luminometer cuvette (Röhren), and after a 30 minutes resting period the agonist was injected at double concentration, both for calcium experiments and for gene expression measurements. To test for differential transcript levels, plants were treated with the chemicals for 1h, 3h, 6h and 9h. The final concentration of the calcium agonists tested were 500 µM ATP, 1 mM L-glutamate, 50 mM calcium (II) chloride and 10 µM mastoparan (all from Sigma-Aldrich). For each of the agonists at each timepoint batches of 5 seedlings were chemically treated inside a luminometer cuvette after a 30 min resting period, to exactly emulate conditions used for the calcium measurements. For each sample for gene expression analysis (representing one agonist at one timepoint), 3 separate biological replicates (15 seedlings in total) were pooled before RNA extraction. The whole experiment (involving 4 agonists plus baseline, at 4 different timepoints) was performed twice and data presented are averages of these 2 separate experiments.

***In vivo* reconstitution of aequorin and Ca^{2+}-dependent luminescence measurements.** Aequorin reconstitution was performed by floating *Arabidopsis* seedlings on water containing 10 µM coelenterazine 1% [v/v] methanol (Biosynth). Plants were left in the dark from 12 to 24 h at 20^{o}C before calcium measurements. To measure calcium levels, *Arabidopsis* seedlings were transferred to a luminometer cuvette and inserted into the luminometer sample housing. Following a 30 min resting period, luminescence levels were recorded every 1 sec using a digital chemiluminometer with discriminator and cooled housing unit (Electron Tubes Limited). Luminescence was recorded for 120 sec before injection of the chemical to provide baseline steady-state readings. Discharge was performed at the end of the experiment by injection of an equal volume of 2 M $CaCl_2$, 20% ethanol. Calibration was performed as previously described (Knight *et al.*, 1996).

cDNA preparation and gene expression measurements. A high capacity cDNA reverse transcription kit (Applied Biosystem) was used to reverse transcribe 2 µg of total RNA obtained with a RNeasy Plant Total RNA kit (Qiagen). Quantitative real-time PCR was performed on 5 µL of 1:50 cDNA dilution in a total volume of 15 µL, using an Applied Biosystem 7300 real time PCR machine. Relative expression levels of *EDS1* (At3g48090) and *ICS1* (At1g74710) were tested with Fast Start SYBR Green Master Mix with ROX using the following primers: *EDS1* Fw 5'-ACCTAACCGAGCGCTATCAC-3', *EDS1* Rev 5'-

TTGTCCGGATCGAAGAAATC-3', *ICS1* Fw 5'-CAAATCTCAACCTCCGTCGT-3', *ICS1* Rev 5'-AATCAATTGCTCCGATTTGC-3'. Levels were normalised to the endogenous levels of the *PEX4* housekeeping gene (At5g25760), and the primers used were *PEX4* Fw 5'-TCATAGCATTGATGGCTCATCCT-3', *PEX4* Rev 5'-ACCCTCTCACATCACCAGATCTTAG-3'. Experiments were performed in optical 96-well plates, with eight technical replicates for each sample. Relative quantification was performed by the $\Delta\Delta C_t$ method (Livak & Schmittgen, 2001), the values obtained representing the relative quantitation (RQ) estimates, and the error bars, representing RQ_{MAX} and $RQ_{MIN,}$ were calculated as described previously (Knight *et al.*, 2009). The algorithm used is described in Relative Quantitation (RQ) Algorithms in Applied Biosystems Real-Time PCR Systems Software (Applied Biosystems Real-Time PCR Systems, 2007).

Differential equations for modelling gene expression. MNNCC_ described in the text is referred to as MNNCCb in the following equations for the clarity of notation. Both b in the equations and _ in the text refer to no binding of any protein to CaM.

$$\frac{d[mRNA_{EDS1}]}{at} = \frac{V_{EDS1}^{\max}\frac{[MNNCCb]}{k_{EDS1,MNNCCb}}\frac{[DR]}{k_{EDS1,DR}}}{(1+\frac{[MNNCCb]}{k_{EDS1,MNNCCb}})(1+\frac{[DR]}{k_{EDS1,DR}})(1+\frac{[MNNCCX]}{k_{EDS1,MNNCCX}})} - k_{EDS1,decay}[mRNA_{EDS1}] \quad \textbf{(eq.1)}$$

$$\frac{d[mRNA_{ICS1}]}{at} = \frac{V_{ICS1}^{\max}\frac{[MNNCCY]}{k_{ICS1,MNNCCY}}\frac{[mRNA_{EDS1}]}{k_{ICS1,MNNCCb}}\frac{[DR]}{k_{ICS1,DR}}}{(1+\frac{[MNNCCY]}{k_{ICS1,MNNCCY}})(1+\frac{[mRNA_{EDS1}]}{k_{ICS1,MNNCCb}})(1+\frac{[DR]}{k_{ICS1,DR}})} - k_{ICS1,decay}[mRNA_{ICS1}] \quad \textbf{(eq 2)}$$

$$\frac{d[DR]}{at} = \frac{V_{DR}^{\max}\frac{[mRNA_{ICS1}]}{k_{DR,ICS1}}}{(1+\frac{[mRNA_{ICS1}]}{k_{DR,ICS1}})} - k_{DR,decay}[DR] \quad \textbf{(eq. 3)}$$

$[mRNA_{EDS1}]$ and $[mRNA_{ICS1}]$ are the transcript concentration of $EDS1$ and $ICS1$, respectively. $[DR]$ is the concentration of $ICS1$ downstream. $[MNNCCb]$, $[MNNCCX]$ and $[MNNCCY]$ are the concentration of the active complexes of calcium signals, $4Ca^{2+}$-CaM, $4Ca^{2+}$-CaM-CAMTA3 and $4Ca^{2+}$-CaM-CBP60g , respectively. $k_{EDS1,MNNCCX}$ is the binding

affinity of CAMTA3 to DNA for $EDS1$ gene expression. All other $k_{\alpha,\beta}$ symbols in the first term of equations 1-3 have the same meaning. $k_{EDS1,decay}$, $k_{ICS1,decay}$ and $k_{DR,decay}$ are the first-order decay rate for $mRNA_{EDS1}$, $mRNA_{ICS1}$ and DR, respectively. $[MNNCCb]$, $[MNNCCX]$ and $[MNNCCY]$ are computed using the upper pane of Fig. 3. The binding of CAMTA3 with calmodulin and Ca^{2+} generates 33 binding reactions and 18 different binding complexes(Liu *et al.*, 2015). Following the analysis previously developed (Liu *et al.*, 2015), the binding of both CAMTA3 and CBP60g with calmodulin and Ca^{2+} generates 54 binding reactions and 27 different binding complexes. In addition, there are a large number of different Ca^{2+}/CaM binding proteins (Reddy *et al.*, 2011; Poovaiah *et al.*, 2013) in plant cells. In addition to CAMTA3 and CBP60g, any other calmodulin binding proteins or transcription factors can be included in the model. Because other calmodulin binding proteins or transcription factors can compete for the binding of calmodulin, they affect the concentrations of the active complexes of calcium signals, $4Ca^{2+}$-CaM, $4Ca^{2+}$-CaM-CAMTA3 and $4Ca^{2+}$-CaM-CBP60g. Therefore, different numbers of other calmodulin binding proteins or transcription factors affect the searched parameter values. The parameters shown in Table S1 corresponds to 100 other calmodulin binding proteins or transcription factors in the model. For the sake of simplicity and due to the lack of biological knowledge on other calmodulin binding proteins, we consider that these 100 other calmodulin binding proteins or transcription factors have the same binding affinity with calmodulin and they have the same concentration. How the other parameters are searched is included in Table S1.

Numerical Method. The model was implemented using simulator Berkeley Madonna (www.berkeleymadonna.com). Rosenbrock (Stiff) method was used with a tolerance of 1.0e-5. Much smaller tolerances (1.0e-6 to 1.0e-8) were also tested and the numerical results show that further reduction of tolerances did not improve the accuracy of numerical results. To study how a calcium signature induces gene expression, the system of ordinary differential equations was settled at a steady state using the average Ca^{2+} concentration of the control experiment as an input before a calcium signature was introduced. Thus, the steady-state values of all concentrations computed using the average Ca^{2+} concentration of the control experiment as an input are the initial values of all concentrations, as shown in

the computational code, Table S2. When a calcium signature was introduced, the response of the system of ordinary differential equations was calculated using the experimentally measured time-dependent Ca^{2+} concentration (Fig. 1) as an input.

Since this work studies how a calcium signature induces gene expression, the initial values of all concentrations are set to be the steady-state values corresponding to the Ca^{2+} concentration of the control experiment. During the model development, we tested the effects of initial values on modelling results. For the model parameters described in Table S1 and using the average Ca^{2+} concentration of the control experiment as an input, the interactions of Ca^{2+}, CaM, CAMTA3, CBP60g and 100 other proteins establish a steady state very quickly (<10s) from any initial value. Thus, modelling results are similar for all initial values for these interactions. However, for the gene expression described by eq.1, 2 and 3, response of gene expression to a calcium signature depends on initial values, and therefore the initial values in eq. 1, 2 and 3 must be set to be the respective steady-state values using the average Ca^{2+} concentration of the control experiment as an input.

Results

Using the calcium agonist mastoparan to establish the relationship between different calcium signatures and specific gene expression responses.

To initially establish the relationship between calcium signatures and calcium-dependent gene expression, we treated Arabidopsis seedlings with the known calcium agonist mastoparan (Fig. 1a,b). Calcium measurements were performed using the recombinant aequorin method (Knight & Knight, 1995). The genes *EDS1* and *ICS1* encode key components of the salicylic acid biosynthetic pathway, required for response to pathogens (Zhang *et al.*, 2010; Zhang *et al.*, 2014). We therefore initially tested the effect of the calcium signature generated by mastoparan upon *EDS1* and *ICS1* transcript expression levels which were quantified by using real-time PCR (Fig. 2). Mastoparan treatment induced *ICS1* gene expression at 3 hours by approximately 37 fold (Fig. 2a) whereas the same treatment only induced a much more modest (approximately 2-3 fold) increase in *EDS1* gene expression (Fig. 2b). The kinetics of expression were also different in both cases, for *ICS1* expression peaked already at 3h and declined relatively slowly until 9h. In contrast, for *EDS1*, maximal induction was achieved at 3h, declining again by 6h. We then used these data to elucidate of

241 the relationship between calcium signatures and expression responses of *EDS1* and *ICS1* by
242 modelling the information flow from calcium signals to *EDS1* and *ICS1* gene expression.
243
244 **A dynamic model for the information flow from calcium signals to gene expression.**
245 Experimental data accumulated over many years have shown that expression of *EDS1* and
246 *ICS1* is regulated by the transcription factors CAMTA3 and CBP60g, respectively (Du *et al.*,
247 2009; Wang *et al.*, 2009; Zhang *et al.*, 2010; Wang *et al.*, 2011). In addition, it has been
248 established experimentally that there is a regulatory network involving *EDS1* and *ICS1*
249 expression as well as their downstream response (Zhang *et al.*, 2014). In this network, *EDS1*
250 and *ICS1* expression and their downstream response are all mutually regulated. Specifically,
251 *EDS1* expression is positively regulated by both EDS1 upstream and ICS1 downstream, but it
252 is negatively regulated by the CAMTA3 transcription factor (Zhang *et al.*, 2014). *ICS1*
253 expression is promoted by *EDS1* expression since EDS1 is an upstream component of *ICS1*
254 expression (Zhang *et al.*, 2014). *ICS1* expression is also positively regulated by both ICS1
255 downstream and the CBP60g transcription factor (Zhang *et al.*, 2014). Since both CAMTA3
256 and CBP60g have CaM binding domains, it has been demonstrated that Ca^{2+} signals regulate
257 the network of *EDS1* and *ICS1* expression and their downstream response (Zhang *et al.*,
258 2014). Taking all these facts into account, Fig. 3 summarises the dynamical model for
259 establishing information flow from calcium signals to *EDS1* and *ICS1* gene expression.
260 The model shown in Fig. 3 includes the fact that CAMTA3 has a calmodulin binding
261 site (Finkler *et al.*, 2007). Since CaM has two pairs of Ca^{2+}-binding EF-hand domains located
262 at the N-and C-terminus respectively, interactions of Ca^{2+}-CaM generate 9 different binding
263 complexes via 12 elementary binding processes, and interactions of Ca^{2+}-CaM and CAMTA3
264 generate 18 different binding complexes via 33 elementary binding processes (Liu *et al.*,
265 2015). Similarly, interactions between Ca^{2+}-CaM and CBP60g also generate 18 different
266 binding complexes, 9 of which are Ca^{2+}-CaM only complexes and are the same as those in
267 interactions of Ca^{2+}-CaM and CAMTA3. Therefore, 9 new complexes are generated for
268 interactions between Ca^{2+}-CaM and CBP60g. In addition, plant cells contain a relatively
269 large number of other Ca^{2+}/CaM binding proteins (Reddy *et al.*, 2011; Poovaiah *et al.*, 2013),
270 and these must be taken into account as they compete with CAMTA3 and CBP60g for CaM.
271 Each of these Ca^{2+}/CaM binding proteins can be analysed using the same method developed
272 for interactions of Ca^{2+}-CaM and CAMTA3 (Liu *et al.*, 2015). For each additional CaM binding

protein, 9 new binding complexes are generated. Thus, for *n* CaM binding proteins there are $9(n+1)$ binding complexes. Published experimental measurements have shown that $4Ca^{2+}$-CaM is the active CaM-Ca^{2+} binding complex (Pifl *et al.*, 1984). Therefore, our model assumes that the $4Ca^{2+}$-CaM-TF complex is the active complex for gene expression responses (Pifl *et al.*, 1984; Liu *et al.*, 2015). Thus, for CAMTA3 and CBP60g, the active complexes for gene expression response are assumed to be $4Ca^{2+}$-CaM-CAMTA3 and $4Ca^{2+}$-CaM-CBP60g, respectively.

The regulatory network upstream of *EDS1* gene is composed of many components, which are regulated by Ca^{2+} signals (Zhang *et al.*, 2014). *EDS1* expression is promoted by the upstream part of this network (Zhang *et al.*, 2014). For model development, we simplified the regulation of *EDS1* gene expression by the upstream components into a single regulatory relationship that is the activation of *EDS1* gene expression by Ca^{2+} signals. Since experimental measurements have shown that $4Ca^{2+}$-CaM is the active CaM and Ca^{2+} binding complex (Pifl *et al.*, 1984), we assume the $4Ca^{2+}$-CaM complex is the active signal that positively regulates *EDS1* gene expression from the upstream part of the network (Zhang *et al.*, 2014). In addition, we simplified the network downstream of *ICS1* into a single response component, DR (downstream response). The transcription factor CAMTA3 inhibits *EDS1* gene expression, and DR activates *EDS1* gene expression (Zhang *et al.*, 2014). The expression of *ICS1* is positively-regulated by EDS1, CBP60g transcription factor and DR (Zhang *et al.*, 2014). Thus, the interaction of EDS1, ICS1 and DR forms the regulatory network shown in Fig. 3.

Fig. 3, therefore, describes the information flow from calcium signatures to *EDS1* and *ICS1* gene expression. The complexity of this information transduction process is multifaceted. Our model (Fig. 3) has included the following aspects. Firstly, transient changes of Ca^{2+} concentration are converted into transient active complexes following the stoichiometry and binding mechanism of Ca^{2+}, CaM, CAMTA3 and CBP60g. Secondly, a large number of other CaM-binding proteins can also bind with CaM. We have included the effects of other CaM-binding proteins in our model. Thirdly, the interaction of EDS1, ICS1 and DR forms a regulatory network. Fourthly, after being converted into the 3 active complexes of (1) $4Ca^{2+}$-CaM; (2) $4Ca^{2+}$-CaM-CAMTA3 and (3) $4Ca^{2+}$-CaM-CBP60g, Ca^{2+} signals have multiple effects on the *EDS1* and *ICS1* expression by regulating the network upstream of *EDS1* and the CAMTA3 and CBP60g transcription factors. Thus, when a calcium signature

occurs, transient changes of Ca^{2+} concentration dynamically regulate the response of *EDS1*, *ICS1* and DR in a complex and nonlinear manner. The dynamic model (Fig. 3) integrates a wide range of knowledge about the information flow from Ca^{2+} signatures to expression of *EDS1* and *ICS1*. To establish the parameters of this model, we compared the output of the model in terms of mastoparan-induced *EDS1* and *ICS1* expression responses to our experimental observations of gene expression (Fig. 2a,b).

Modelling results reproduce experimental observations.

Fig. 5 shows an example of fitting the dynamic model (Fig. 3) to the experimentally measured transcript fold changes for both *EDS1* and *ICS1* genes (Fig. 2) in response to the calcium signature induced by 10 µM mastoparan (Fig. 1a,b). For the unmeasured Ca^{2+} concentration, we assume that Ca^{2+} concentration approaches the original steady state (Fig. 4a). For simplicity, we consider that Ca^{2+} concentration linearly decreases to its steady state within τ_c (Fig. 4a), defined as the time required for a calcium signature to return to its steady state. For different values of τ_c, Fig. 4b,c,d show the responses of the concentrations of the three active complexes ($4Ca^{2+}$-CaM-CAMTA3, $4Ca^{2+}$-CaM-CBP60g and $4Ca^{2+}$-CaM, respectively). Importantly, Fig. 5a,b show that, although different values of τ_c always generate similar temporal trends for transcript fold changes for both *EDS1* and *ICS1*, different values of τ_c do quantitatively affect modelling results. In Fig. 5, the values of τ_c in the range of 2-3 hours generate results which best fit to experimental observations. Therefore, Fig. 4 and Fig. 5 reveals how the calcium signature induced by 10 µM mastoparan is decoded to generate specific responses of *EDS1* and *ICS1* expression. When the mastoparan calcium signature is produced, the transient elevation in intracellular Ca^{2+} concentration is converted into three active complexes that regulate *EDS1* and *ICS1* expression: $4Ca^{2+}$-CaM, $4Ca^{2+}$-CaM-CAMTA3 and $4Ca2^{+}$-CaM-CBP60g. (Fig. 3). For the calcium signature induced by 10 µM mastoparan (Fig. 1a,b), transient elevation in intracellular Ca^{2+} concentration is limited to a relatively small range and the maximum fold change relative to the steady-state Ca^{2+} concentration is less than 10 fold during the lifetime of this calcium signature (Fig. 1a,b). However, due to the action of CaM, CAMTA3 and CBP60g in decoding this calcium signature (Fig. 3), the three active complexes ($4Ca^{2+}$-CaM, $4Ca^{2+}$-CaM-CAMTA3 and $4Ca2^{+}$-CaM-CBP60g) vary their concentrations by a much wider

range and the maximum fold changes relative to their steady-state values and can reach around 2500 fold. Thus, one calcium signature is amplified into three active signals and each of these three amplified signals is capable of regulating *EDS1* or *ICS1* expression response (Fig. 3). In addition, since expression of *EDS1* and *ICS1* forms a network (Fig. 3), the three active signals, which originate from the same calcium signature, interplay via this network. Thus, regulation of *EDS1* and *ICS1* expression by the mastoparan-induced calcium signature (Fig. 5a,b) is highly nonlinear due to these interactions of the three amplified active signals (Fig. 4b,c,d). Since the dynamic model (Fig. 3) can reproduce experimental data, we conclude that the model captures the main features of the information flow from calcium signals to *EDS1* and *ICS1* gene expression.

The next step was to test whether, now that it was established and parameterised, the model could predict *EDS1* and *ICS1* gene expression responses to other calcium signatures (Fig. 1), as gauged by comparing model-derived predictions to empirically-determined gene expression data.

Predictions of how three different calcium signatures will be decoded match empirical observations of gene expression responses.

To predict the relationships between calcium signatures and gene expression responses we used the other three experimentally measured calcium signatures induced by treatments with the calcium agonists ATP, extracellular calcium and glutamate (Fig. 1). These empirically-derived calcium signatures were used, as model inputs, to calculate the predicted transcript fold responses for both *EDS1* and *ICS1* gene expression without changing any parameters (Fig. 6a,b,c,d,e,f). As Ca^{2+} concentrations of different calcium signatures at the end of the experimentally measured data are different (Fig. 1), it is plausible that different calcium signatures may have different values of τ_c. Thus, we generated predictions for a range of τ_c values. Fig. 6 shows that the modelling predictions on the transcript fold responses for both *EDS1* and *ICS1* to the 3 calcium signatures (Fig. 1) are in agreement with experimental fold changes and temporal trends. Experimental data show that whilst a 10 µM mastoparan treatment induced large fold change in *ICS1* gene expression (around 37 fold at 3 hours, Fig. 2a) the other three calcium signatures could only induce much smaller fold changes in *ICS1* gene expression (approximately maximum 5 fold

at 6 hours, Fig. 6a). As can be seen in Fig. 6a,c,e the model indeed predicts that the other three calcium signatures in Fig. 1 would indeed only generate relative small fold change for *ICS1* expression (around maximum 5 fold at 6 hours (see the curve corresponding to τ_c = 7300s in Fig. 6a). The model predicts that the 3 calcium signatures shown in Fig. 1 would generally generate small fold changes for *EDS1* expression (Fig. 6b,f). Our experimental data indeed confirmed that the three calcium signatures always generate small transcript fold changes for *EDS1* gene expression (around maximum 3 fold at 1 hour, Fig. 6b,f). The model also correctly predicted that the calcium signature triggered by glutamate (Fig. 1) would not induce *EDS1* expression at all, which was confirmed by experimental observation (Fig. 6d). Therefore, modelling predictions for both *EDS1* and *ICS1* expression are in agreement with experimental observations.

Additionally, the model was able to predict the temporal trends of the transcript fold responses for both *EDS1* and *ICS1* gene expression to the three test calcium signatures. Experimental data show that fold change of *EDS1* expression from 1 hour to 9 hours generally does not display temporal variation (Fig. 6b,d,f) for the three calcium signatures. The model correctly predicts that *EDS1* expression for the three calcium signatures generally does not change temporally from 1 hour to 9 hours (Fig. 6b,d,f). Experimental data show that the calcium signatures induced by both ATP and glutamate result in *ICS1* transcript fold change generally decreasing from 1 hour to 9 hours (Fig. 6c,e) whereas the calcium signature induced by extracellular Ca^{2+} results in *ICS1* transcript fold change generally increasing from 1 hour to 9 hours (Fig. 6a). Again, the model was able to predict similar temporal *ICS1* transcript fold change trends for the 3 test calcium signatures (Fig. 6a,c,e). Taken together, the model (Fig. 3) was thus able to correctly predict the temporal trends of the transcript fold responses for both *EDS1* and *ICS1* gene expression to the three test calcium signatures. Therefore, our results have demonstrated that a novel integrated experimental and modelling study, in which a wide range of biological knowledge in the literature is integrated with our own experimental data, can elucidate and predict the response of *EDS1* and *ICS1* gene expression to different calcium signatures.

Discussion

Here we describe a novel integrated experimental and modelling study, in which a wide range of biological knowledge from the literature was integrated with our experimental data. This enabled us to establish the information flow from calcium signatures to the expression of specific calcium-regulated genes in plant cells. Our experimental data show that different calcium signatures can generate specific *EDS1* and *ICS1* gene expression responses (Fig. 2 and 6). The biological knowledge accumulated over many years in the literature was abstracted into a dynamic model (Fig. 3). The model was parameterised by using experimentally measured parameters in the literature (Liu *et al.*, 2015) and by fitting the model to the experimentally measured transcript fold changes for both *EDS1* and *ICS1* genes in response to the calcium signature induced by 10 µM mastoparan (Fig. 1). We further demonstrated that the model developed in this study was always able not only to reproduce experimental observations (Fig. 4, 6, S1, S2 and S3), but also to make predictions that are validated experimentally (Fig. 6, S4, S5, S6). Therefore, a combined experimental and modelling study is able to reveal how different calcium signatures are decoded to specific responses gene expression. Relationships between calcium signatures and responses of *EDS1* and *ICS1* gene expression can therefore be elucidated and predicted. Our work also establishes how calcium signatures are decoded by Arabidopsis to generate the expression responses of two genes (*EDS1* and *ICS1*) important in plant immunity. Our combined modelling and experimental analysis reveals the complexity of this decoding process. Calcium signals are amplified into three active signals via Ca^{2+} and CaM interaction, and via both CAMTA3 and CBP60g transcription factors (the 3 signals being: $4Ca^{2+}$-CaM, $4Ca^{2+}$-CaM-CAMTA3 and $4Ca^{2+}$-CaM-CBP60g). In addition, since expression of *EDS1* and *ICS1* forms a network (Fig. 3), the three active signals, which originate from the same calcium signature, interplay via this network. Thus, regulation of *EDS1* and *ICS1* expression (Fig. 2, 5 and 6) by the calcium signatures is highly nonlinear due to the interactions of these three amplified active signals (Fig. 4b,c,d). Therefore, specific responses of *EDS1* and *ICS1* expression to the calcium signatures are due to nonlinear interactions of the three amplified active signals originating from the same calcium signature. Because our combined experimental and modelling study is able to establish the relationships between gene expression responses and calcium signatures, it supports the concept that calcium signalling plays a vital role in plant immunity.

Calcium signatures are generally relatively short lived increases in calcium concentration. As a dynamically transient signal, a calcium signature generally tends to return to a steady state level. This level can be the same concentration as before the start of the transient, or can be a different steady state level. Traditionally, much attention has been paid to the characteristics of a calcium signature within a relatively short period after initiation. How a calcium signature returns to a steady state has been largely ignored. Our work shows that the time required for a calcium signature to return to a steady state, τ_c, is a factor which quantitatively affects the subsequent gene expression response. This demonstrates that our combined experimental and modelling methodology is capable of identifying unknown factors about the decoding of calcium signatures. As the key properties of the calcium signatures important in mediating specific gene expression responses were not intuitive this necessitated a mathematical modelling approach.

Whilst our combined experimental and modelling methodology is capable of predicting both the fold change and temporal pattern for *EDS1* and *ICS1* gene expression (Fig. 5 and 6), our model (Fig. 3) cannot perfectly fit the expression pattern of *EDS1* and *ICS1* for agonist mastoparan (Fig. 5) nor perfectly predict the expression pattern of both genes for other agonists (Fig. 6). For example, whilst Fig. 5 shows that *ICS1* gene expression for agonist mastoparan is induced at 3600s according to experimental measurements, the computed fold change of *ICS1* transcripts does not increase until 5200s. Once the time reaches 5200s, the fold change starts to rapidly increase in the model fitting. When a calcium signal is produced, a change in gene expression cannot occur instantaneously, as the transcriptional pre-initiation complex (containing specific transcription factors e.g. CAMTA3, general transcription factors, mediator and RNA polymerase) needs to be recruited and assembled and an elongation complex needs to form to allows transcription of the coding region (Lee and Young, 2000). Therefore, a time delay between calcium signal and gene expression response needs to be considered (Liu et al., 2015). Since the exact subcellular locations of both Ca^{2+} and the components for both *EDS1* and *ICS1* expression such as transcription factor, Mediator and RNA polymerase have not been experimentally determined, a single parameter, included in Table S1, is used to describe the time delay between calcium signal and gene expression response. Fig. S7 shows that increasing the time delay of either *ICS1* or *EDS1* gene expression increases the induction time of *ICS1* or

EDS1 gene expression accordingly. For example, increasing the time delay of *ICS1* from 3600s to 7200s increases the induction time of *ICS1* gene expression from 3600s to 7200s. Fig. S8 shows that a time delay between 5000s and 9000s for *ICS1* gene expression generates best-fitting of the fold changes of *ICS1* transcripts. However, a time delay between 200s and 1000s for *EDS1* gene expression generates best-fitting of the fold changes of *ICS1* transcripts. Therefore, together Fig. S7 and S8 reveals that time delay is an important parameter for determining when *EDS1* and *ICS1* expression is induced. Although time delay can affect modelling results, we have not found such a combination of the two time delays for *EDS1* and *ICS1* expression that a perfect fitting or prediction can be generated. Since time delay between calcium signal and gene expression response is defined by a single parameter, once time delay has elapsed, gene expression immediately starts to rapidly increase (Fig. 5) following a rapid increase in calcium concentration at the beginning of a calcium signature (Fig. 1). However, it is plausible that the availability of the components required for gene expression such as transcription factors, Mediator and RNA polymerase at the location of gene expression is also important for gene expression response. Thus, to improve model fitting and prediction, the model (Fig. 3) needs to be further developed to include the exact subcellular locations of Ca^{2+} and the components for gene expression such as transcription factor, Mediator and RNA polymerase. However, constructing a model to explicitly include spatial setting is currently impossible as such experimental data are unavailable. Recently, Yuan et al. (2017) discussed that detection of the exact subcellular locations of Ca^{2+} is important for future research. Combining a high resolution of spatial Ca^{2+} distribution with experimentally-measured locations of components required for the expression of *EDS1* and *ICS1* such as transcription factors, Mediator and RNA polymerase, future research should be able to more precisely predict the dynamics of gene expression.

Experimental data accumulated over many years have revealed multiple levels of complexities in decoding calcium signals in plant cells (Edel et al. 2017; Yuan et al. 2017). Plants cells possess four main types of Ca^{2+} sensor proteins to relay or decode Ca^{2+} signalling: CaM, CaM-like proteins (CMLs), calcineurin B-like proteins (CBLs) and Ca^{2+}-dependent protein kinases (CDPKs or CPKs) (Yuan et al. 2017). These proteins relay or decode calcium signals at both transcriptional and post-translational levels (Yuan et al. 2017). Our research presented in this work has focused on an example at the transcriptional

level specifically. Using two important genes in plant immunity, *EDS1* and *ICS1*, as an example, this work demonstrates that the specific responses of gene expression to calcium signatures can be elucidated and predicted by a combined experimental and modelling analysis and that a cellular mechanism for decoding calcium signatures can be identified (Fig. 3). In principle, the upper pane of Fig. 3 could be used to study the interactions of Ca^{2+} and any Ca^{2+} and/or CaM binding protein. For example, during symbiosis, the Ca^{2+}/CaM-dependent protein kinase (CCaMK) (Gleason et al. 2006; Patil et al 1995) plays an essential role in the interpretation of symbiotic Ca^{2+} signalling in the nucleus for the establishment of symbiotic responses (Yuan et al. 2017). Thus, to explore symbiotic responses, CCaMK could be explicitly included in the upper pane of Fig. 3 to investigate how CCaMK interacts with Ca^{2+} and calmodulin to generate an active signal for promoting the phosphorylation of a substrate. Similarly, in principle, the lower pane of Fig. 3 can be used to study the regulation of any biological system by any active Ca^{2+} signal. For example, the active signal generated by the interaction of Ca^{2+}, CaM and CCaMK, which can be computed after incorporating CCaMK into the upper pane of Fig. 3, can be used to investigate how CCaMK promotes the phosphorylation of a substrate if the regulatory mechanism of the phosphorylation process can be established the lower pane of Fig. 3 following experimental data. In addition, it is also possible to study the interplay between the post-translational level and transcriptional level, e.g. by establishing how CCaMK, CAMTA3 and CBP60g compete for the binding with CaM. Thus, the methodology developed here can be further developed to study the decoding of calcium signatures in both transcriptional and post-translational levels, and to determine the decoding mechanisms of calcium signatures at both levels in plant cells.

Acknowledgements

This work was funded by an EU-funded Initial Training Network (ITN) CALIPSO GA 2013–607607.

Author contributions

G.L., J.L. and M.R.K. designed the experiments and the model, analysed the data and wrote the paper; G.L. conducted the experiments; J.L. developed modelling analysis.

References

Allen GJ, Chu SP, Harrington CL, Schumacher K, Hoffmann T, Tang YY, Grill E, Schroeder JI. 2001. A defined range of guard cell calcium oscillation parameters encodes stomatal movements. *Nature* **411**: 1053-1057.

Berridge MJ, Bootman MD, Roderick HL. 2003. Calcium signalling: Dynamics, homeostasis and remodelling. *Nature Reviews Molecular Cell Biology* **4**: 517-529.

Bickerton PD, Pittman JK 2012. Calcium Signalling in Plants. *eLS*: John Wiley & Sons, Ltd,., Chichester.

Clapham DE. 2007. Calcium signaling. *Cell* **131**: 1047-1058.

Dodd AN, Kudla J, Sanders D. 2010. The language of calcium signaling. *Annu Rev Plant Biol* **61**: 593-620.

Du L, Ali GS, Simons KA, Hou J, Yang T, Reddy ASN, Poovaiah BW. 2009. Ca2+/calmodulin regulates salicylic-acid-mediated plant immunity. *Nature* **457**: 1154-1158.

Edel KH, Marchadier E, Brownlee C, Kudla J, Hetherington AM. 2017. The evolution of calcium-based signalling in plants. *Current Biology* **27**: R667-R679.

Finkler A, Ashery-Padan R, Fromm H. 2007. CAMTAs: calmodulin-binding transcription activators from plants to human. *FEBS Lett* **581**: 3893-3898.

Galon Y, Aloni R, Nachmias D, Snir O, Feldmesser E, Scrase-Field S, Boyce JM, Bouche N, Knight MR, Fromm H. 2010. Calmodulin-binding transcription activator 1 mediates auxin signaling and responds to stresses in Arabidopsis. *Planta* **232**: 165-178.

Gleason C, Chaudhuri S, Yang T, Munoz A, Poovaiah BW, Oldroyd GED. 2006. Nodulation independent of rhizobia induced by a calcium-activated kinase lacking autoinhibition. *Nature* **441**: 1149-1152.

Galon Y, Nave R, Boyce JM, Nachmias D, Knight MR, Fromm H. 2008. Calmodulin-binding transcription activator (CAMTA) 3 mediates biotic defense responses in Arabidopsis. *FEBS Lett* **582**: 943-948.

Grant M, Brown I, Adams S, Knight M, Ainslie A, Mansfield J. 2000. The RPM1 plant disease resistance gene facilitates a rapid and sustained increase in cytosolic calcium that is necessary for the oxidative burst and hypersensitive cell death. *Plant Journal* **23**: 441-450.

Hashimoto K, Kudla J. 2011. Calcium decoding mechanisms in plants. *Biochimie* **93**: 2054-2059.

Kim MC, Chung WS, Yun DJ, Cho MJ. 2009. Calcium and calmodulin-mediated regulation of gene expression in plants. *Mol Plant* **2**: 13-21.

Kim MC, Panstruga R, Elliott C, Muller J, Devoto A, Yoon HW, Park HC, Cho MJ, Schulze-Lefert P. 2002. Calmodulin interacts with MLO protein to regulate defence against mildew in barley. *Nature* **416**: 447-451.

Knight H, Knight MR. 1995. Recombinant aequorin methods for intracellular calcium measurement in plants. *Methods Cell Biol* **49**: 201-216.

Knight H, Mugford SG, Ulker B, Gao D, Thorlby G, Knight MR. 2009. Identification of SFR6, a key component in cold acclimation acting post-translationally on CBF function. *Plant J* **58**: 97-108.

Knight H, Trewavas AJ, Knight MR. 1996. Cold calcium signaling in Arabidopsis involves two cellular pools and a change in calcium signature after acclimation. *Plant Cell* **8**: 489-503.

Knight MR, Campbell AK, Smith SM, Trewavas AJ. 1991. Transgenic Plant Aequorin Reports the Effects of Touch and Cold-Shock and Elicitors on Cytoplasmic Calcium. *Nature* **352**: 524-526.

Kudla J, Batistic O, Hashimoto K. 2010. Calcium signals: the lead currency of plant information processing. *Plant Cell* **22**: 541-563.

Lee TI, Young RA. 2000. Transcription of eukaryotic protein-coding genes. *Annual Review of Genetics* **34**: 77–137.

Liu J, Whalley HJ, Knight MR. 2015. Combining modelling and experimental approaches to explain how calcium signatures are decoded by calmodulin-binding transcription activators (CAMTAs) to produce specific gene expression responses. *New Phytol*. **208**: 174–187.

Livak KJ, Schmittgen TD. 2001. Analysis of relative gene expression data using real-time quantitative PCR and the 2(-Delta Delta C(T)) Method. *Methods* **25**: 402-408.

McAinsh MR, Pittman JK. 2009. Shaping the calcium signature. *New Phytol* **181**: 275-294.

Murashige T, Skoog F. 1962. A Revised Medium for Rapid Growth and Bio Assays with Tobacco Tissue Cultures. *Physiol Plant* **15**: 473-497.

Patil S, Takezawa D, Poovaiah BW. 1995. Chimeric plant calcium/ calmodulin-dependent protein kinase gene with a neural visinin-like calcium-binding domain. *Proceedings of the National Academy of Sciences* **92**: 4897-4901.

Pifl C, Plank B, Wyskovsky W, Bertel O, Hellmann G, Suko J. 1984. Calmodulin X (Ca2+)4 is the active calmodulin-calcium species activating the calcium-, calmodulin-dependent protein kinase of cardiac sarcoplasmic reticulum in the regulation of the calcium pump. *Biochim Biophys Acta* **773**: 197-206.

Poovaiah BW, Du L, Wang H, Yang T. 2013. Recent Advances in Calcium/Calmodulin-Mediated Signaling with an Emphasis on Plant-Microbe Interactions. *Plant Physiol* **163**: 531-542.

Ranty B, Aldon D, Cotelle V, Galaud JP, Thuleau P, Mazars C. 2016. Calcium Sensors as Key Hubs in Plant Responses to Biotic and Abiotic Stresses. *Frontiers in Plant Science* **7**, 1-7.

Reddy AS, Ali GS, Celesnik H, Day IS. 2011. Coping with stresses: roles of calcium- and calcium/calmodulin-regulated gene expression. *Plant Cell* **23**: 2010-2032.

Seybold H, Trempel F, Ranf S, Scheel D, Romeis T, Lee J. 2014. Ca2+ signalling in plant immune response: from pattern recognition receptors to Ca2+ decoding mechanisms. *New Phytol* **204**: 782-790.

Tsuda K, Somssich IE. 2015. Transcriptional networks in plant immunity. *New Phytol* **206**: 932-947.

Vlot AC, Dempsey DA, Klessig DF. 2009. Salicylic Acid, a multifaceted hormone to combat disease. *Annu Rev Phytopathol* **47**: 177-206.

Wang L, Tsuda K, Sato M, Cohen JD, Katagiri F, Glazebrook J. 2009. Arabidopsis CaM binding protein CBP60g contributes to MAMP-induced SA accumulation and is involved in disease resistance against Pseudomonas syringae. *PLoS Pathog* **5**: e1000301.

Wang L, Tsuda K, Truman W, Sato M, Nguyen le V, Katagiri F, Glazebrook J. 2011. CBP60g and SARD1 play partially redundant critical roles in salicylic acid signaling. *Plant J* **67**: 1029-1041.

Whalley HJ, Knight MR. 2013. Calcium signatures are decoded by plants to give specific gene responses. *New Phytol* **197**: 690-693.

Yuan P, Jauregui E, Du L, Tanaka K, Poovaiah BW. 2017 Calcium signatures and signaling events orchestrate plant-microbe interactions. *Curr Opin Plant Biol.* **38**: 173-183.

Zhang L, Du L, Shen C, Yang Y, Poovaiah BW. 2014. Regulation of plant immunity through ubiquitin-mediated modulation of Ca(2+) -calmodulin-AtSR1/CAMTA3 signaling. *Plant J* **78**: 269-281.

Zhang Y, Xu S, Ding P, Wang D, Cheng YT, He J, Gao M, Xu F, Li Y, Zhu Z, Li X, Zhang Y. 2010. Control of salicylic acid synthesis and systemic acquired resistance by two members of a plant-specific family of transcription factors. *Proceedings of the National Academy of Sciences* **107**: 18220-18225.

Zipfel C, Oldroyd GED. 2017. Plant signalling in symbiosis and immunity. *Nature* **543**: 328-336.

Figure legends

Fig. 1 Different calcium agonists produce different calcium signatures. Effect upon cytosolic calcium concentration ($[Ca^{2+}]_c$) in *Arabidopsis thaliana* of treatment with either 500µM ATP (ATP); 50 mM extracellular calcium (eCa); 1 mM glutamate (L-Glu); or 10 µM mastoparan. (a) $[Ca^{2+}]_c$ plotted against 1000s, shading around each plot line represents standard error of the mean (n=6 replicates of 5 treated seedlings); (b) $[Ca^{2+}]_c$ plotted against 110-160s to show details of early kinetics in $[Ca^{2+}]_c$), error bars represents standard error of the mean (n=6 replicates of 5 treated seedlings).

Fig. 2 Calcium signature in response to mastoparan induces *ICS1* and *EDS1* gene expression. (a) Fold increase in *ICS1* transcript expression in *Arabidopsis thaliana* in response to 10 µM mastoparan 1, 3, 6 and 9h after start of treatment. (b) Fold increase in *EDS1* transcript expression in *Arabidopsis thaliana* in response to 10 µM mastoparan 1, 3, 6 and 9h after start of treatment. Letters above error bars refer to significant difference ($P<0.05$) between the average CT values for each timepoint/treatment as determined by pairwise t-tests. Below these letters are symbols to denote the significant difference in average CT value compare to baseline expression at that timepoint; $P<0.0005$ (*****),$P<0.005$ (***), $P<0.05$ (*), not significant (ns) as determined by pairwise t-tests.

Fig. 3 A dynamic model for the information flow from calcium signatures to *EDS1* and *ICS1* gene expression. The upper pane describes the interactions of Ca^{2+}, CaM, CAMTA3, CBP60g and other CaM-binding proteins. The interactions of Ca^{2+}-CaM and CAMTA3 have been previously described in detail (Liu et al., 2015). Other interactions are dealt with in the same way as for the interactions of Ca^{2+}-CaM and CAMTA3 (See "A dynamic model for the information flow from calcium signals to gene expression" section). The lower pane describes the regulatory network of *EDS1* and *ICS1* expression (Zhang et al., 2014). We simplified the network downstream of *ICS1* into a single component, downstream response (DR). Black solid lines: mass conversion; red solid lines: regulatory relationships confirmed by experiments; red dash lines: regulatory relationships derived from experiments.

Fig. 4 Dynamic model-fitting to experimental data for calcium signature and gene expression responses to mastoparan. (a) Calcium signature induced by 10 µM mastoparan and how it approaches its steady state. (b) Response of active signal $4Ca^{2+}$-CaM to the calcium signature (MNNCC_: M: CaM; N: 1 Ca^{2+} binding to N-terminus of CaM; C: 1 Ca^{2+} binding to C-terminus of CaM; _: no binding – the regulation of *EDS1* expression by the network upstream of it is assumed to be via an active Ca^{2+} signal ($4Ca^{2+}$-CaM)). (c) Response of active signal $4Ca^{2+}$-CaM-CAMTA3 to the calcium signature (MNNCCX: M: CaM; N: 1 Ca^{2+} binding to N-terminus of CaM; C: 1 Ca^{2+} binding to C-terminus of CaM; X: CAMTA3). (d) Response of active signal $4Ca^{2+}$-CaM-CBP60g to the calcium signature (MNNCCY: M: CaM; N: 1 Ca^{2+} binding to N-terminus of CaM; C: 1 Ca^{2+} binding to C-terminus of CaM; Y: CBP60g). From left to right (i.e. the curve with the colour dark blue, red, green, brown and light blue,

651 respectively) : τ_c =1000s, 3700s, 7300s, 11800s, 15400s, respectively (τ_c is the time
652 required for transient elevation of calcium concentration to re-establish a steady state).
653 Parameters are included in Table S1.

654 **Fig 5.** Comparison of modelled gene expression with experimental data. (a) Comparison of
655 modelled fold changes of *EDS1* transcript with experimental data from *Arabidopsis thaliana*.
656 Curves are the modelling results and the scattered data with error bars are the experimental
657 results. (b) Comparison of modelled fold changes of *ICS1* transcript with experimental data
658 from *Arabidopsis thaliana*. Curves are the modelling results and the scattered data with
659 error bars are the experimental results. Each sub-graph has 5 curves, corresponding to
660 different values of τ_c (the time required for transient elevation of calcium concentration to
661 re-establish a steady state). From bottom to top (i.e. the curve with the colour dark blue,
662 red, green, brown and light blue, respectively): τ_c =1000s, 3700s, 7300s, 11800s, 15400s,
663 respectively. Parameters are included in Table S1.

664 **Fig. 6** Modelling predictions on the transcript fold responses for both *EDS1* and *ICS1* to three
665 calcium signatures and their comparison with experimental observations. (a) to (f) are
666 modelling predictions and their comparison with experimental observations from
667 *Arabidopsis thaliana*. (a) Predicted fold change of *ICS1* transcripts over time in response to
668 the calcium signature induced by extracellular calcium. (b) Predicted fold change of *EDS1*
669 transcripts over time in response to the calcium signature induced by extracellular calcium.
670 (c) Predicted fold change of *ICS1* transcripts over time in response to the calcium signature
671 induced by glutamate. (d) Predicted fold change of *EDS1* transcripts over time in response to
672 the calcium signature induced by glutamate. (e) Predicted fold change of *ICS1* transcripts
673 over time in response to the calcium signature induced by ATP. (f) Predicted fold change of
674 *EDS1* transcripts over time in response to the calcium signature induced by ATP. In (a) to (f)
675 curves are the modelling results and the scattered data with error bars are the experimental
676 results. Letters above error bars refer to significant difference (P<0.05) between the average
677 CT values for each timepoint/treatment as determined by pairwise t-tests. Below these
678 letters are symbols to denote the significant difference in average CT value compare to
679 baseline expression at that timepoint; P<0.0005 (*****), P<0.001 (****), P<0.005 (***),
680 P<0.01 (**), P<0.05 (*), not significant (ns) as determined by pairwise t-tests. In (a) to (f)

each sub-graph has 5 curves, corresponding to different values of τ_c (the time required for transient elevation of calcium concentration to re-establish a steady state). From bottom to top (i.e. the curve with the colour dark blue, red, green, brown and light blue, respectively): τ_c =1000s, 3700s, 7300s, 11800s, 15400s, respectively. Parameters are the same as in Fig. 4 and 5, and they are included in Table S1.

Fig. S1 Comparison of modelled gene expression with experimental data with altered parameters described in Table S1.

Fig. S2 Comparison of modelled gene expression with experimental data with altered parameters described in Table S1.

Fig. S3 Comparison of modelled gene expression with experimental data with altered parameters described in Table S1.

Fig. S4 Modelling predictions on the transcript fold responses for both *EDS1* and *ICS1* with altered parameters described in Table S1.

Fig. S5 Modelling predictions on the transcript fold responses for both *EDS1* and *ICS1* with altered parameters described in Table S1.

Fig. S6 Modelling predictions on the transcript fold responses for both *EDS1* and *ICS1* with altered parameters described in Table S1.

Fig. S7 Effects of the time delay between calcium signal and gene expression response on the dynamics of the fold changes of gene expression.

Fig. S8 Dependence of the difference between the experimental fold change of both *ICS1* and *EDS1* transcripts and the computed counterparts on the delay time between calcium signal and gene expression response.

Table S1 Parameters for modelling and parameter searching.

Table S2 Original code (program) for the modelling analysis.

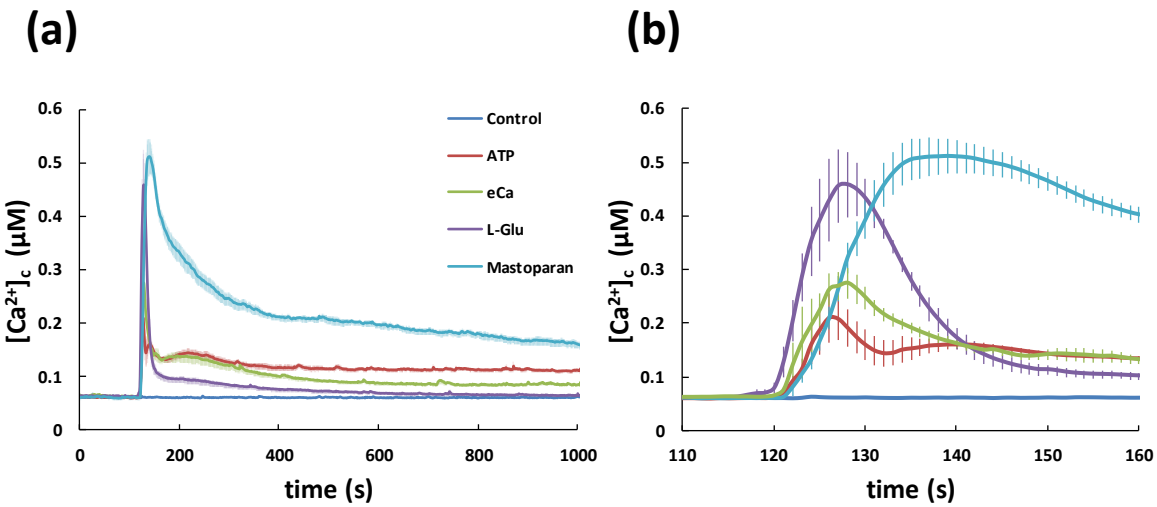
(a)
(b)
Control
ATP
eCa
L-Glu
Mastoparan
[Ca2+]c (μM)
time (s)
0
0.1
0.2
0.3
0.4
0.5
0.6
0
200
400
600
800
1000
110
120
130
140
150
160

FIGURE 1

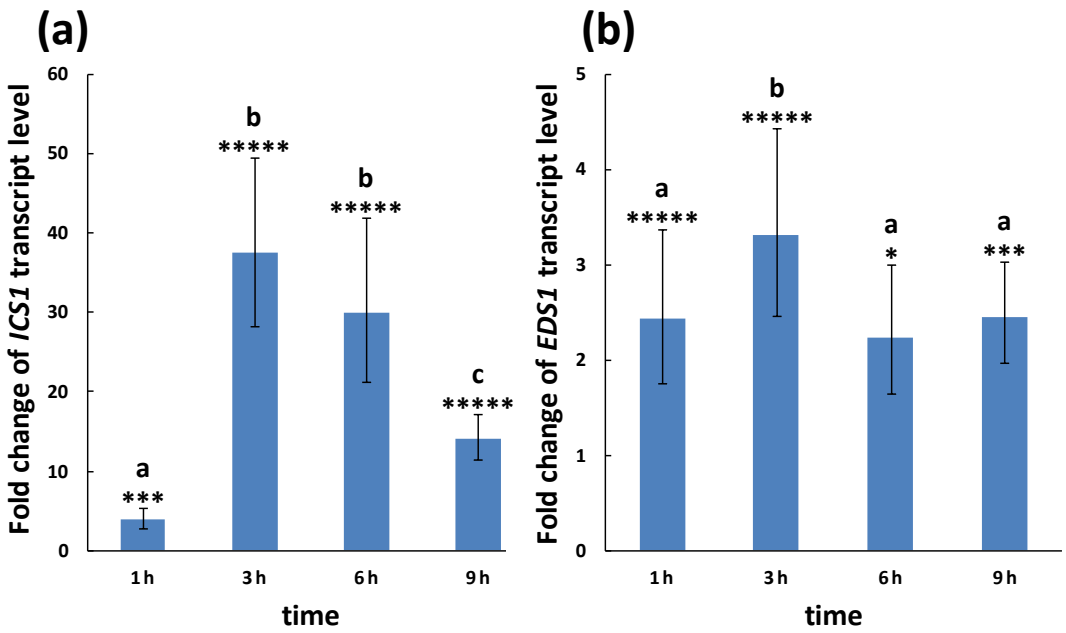
(a)
Fold change of ICS1 transcript level
60
50
40
30
20
10
0
a
***
b
*****
b
*****
c
*****
1 h
3 h
6 h
9 h
time
(b)
Fold change of EDS1 transcript level
5
4
3
2
1
0
a
*****
b
*****
a
*
a
***
1 h
3 h
6 h
9 h
time

FIGURE 2

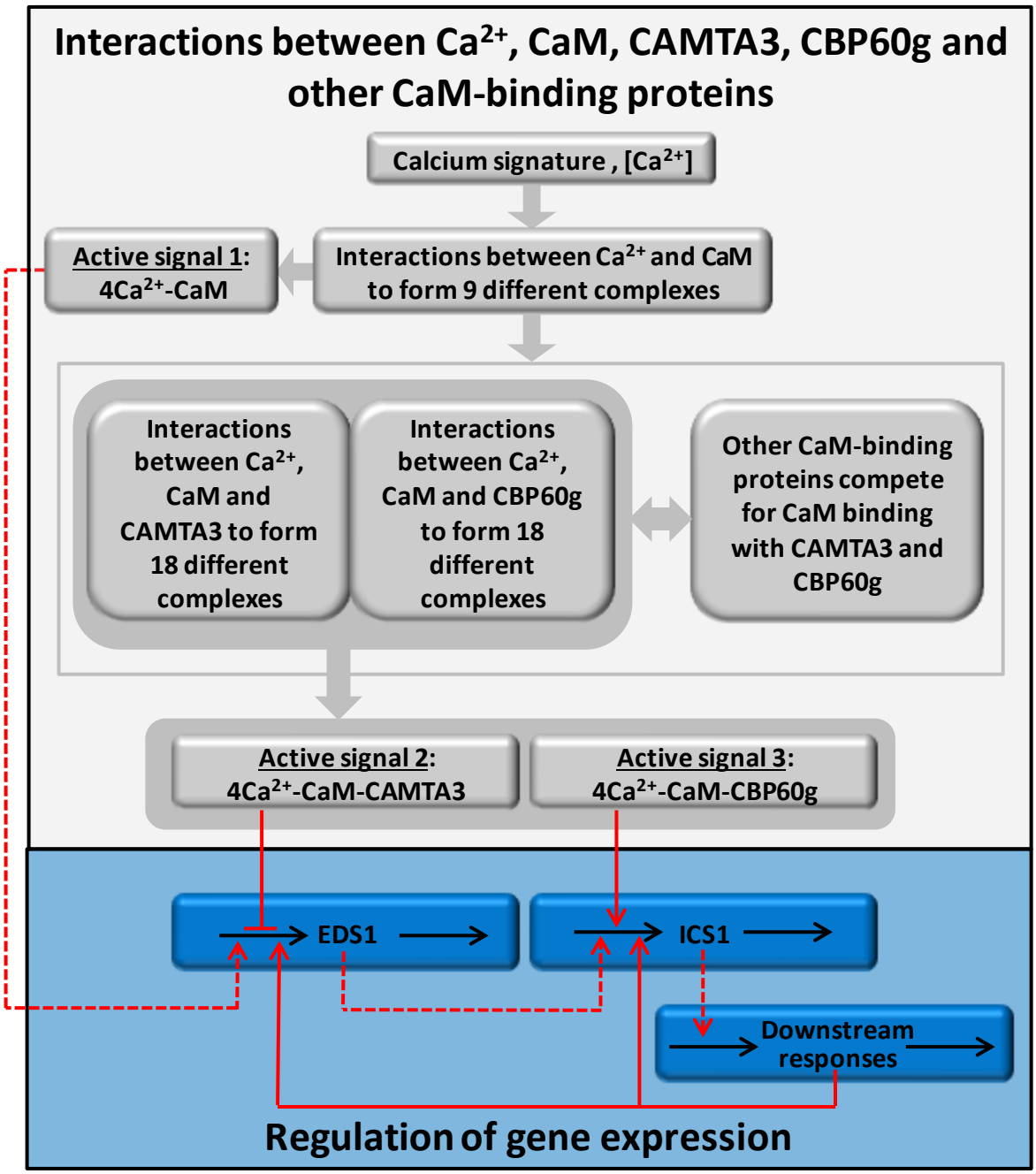
Interactions between Ca2+, CaM, CAMTA3, CBP60g and other CaM-binding proteins
Calcium signature , [Ca2+]
Interactions between Ca2+ and CaM to form 9 different complexes
Active signal 1: 4Ca2+-CaM
Interactions between Ca2+, CaM and CAMTA3 to form 18 different complexes
Interactions between Ca2+, CaM and CBP60g to form 18 different complexes
Other CaM-binding proteins compete for CaM binding with CAMTA3 and CBP60g
Active signal 2: 4Ca2+-CaM-CAMTA3
Active signal 3: 4Ca2+-CaM-CBP60g
EDS1
ICS1
Downstream responses
Regulation of gene expression

FIGURE 3

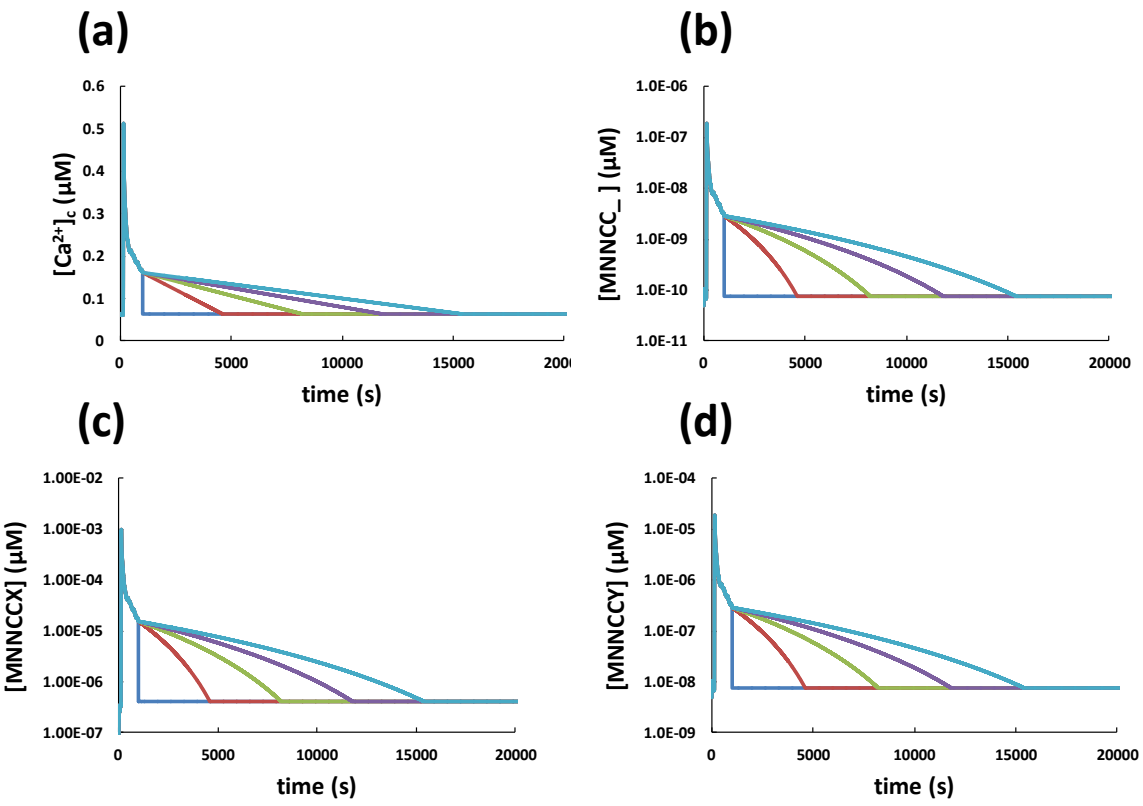
(a)
[Ca2+]c (μM)
0.6
0.5
0.4
0.3
0.2
0.1
0
0
5000
10000
15000
time (s)
(b)
[MNNCC_] (μM)
1.0E-06
1.0E-07
1.0E-08
1.0E-09
1.0E-10
1.0E-11
0
5000
10000
15000
20000
time (s)
(c)
[MNNCCX] (μM)
1.00E-02
1.00E-03
1.00E-04
1.00E-05
1.00E-06
1.00E-07
0
5000
10000
15000
20000
time (s)
(d)
[MNNCCY] (μM)
1.0E-04
1.0E-05
1.0E-06
1.0E-07
1.0E-08
1.0E-09
0
5000
10000
15000
20000
time (s)

FIGURE 4

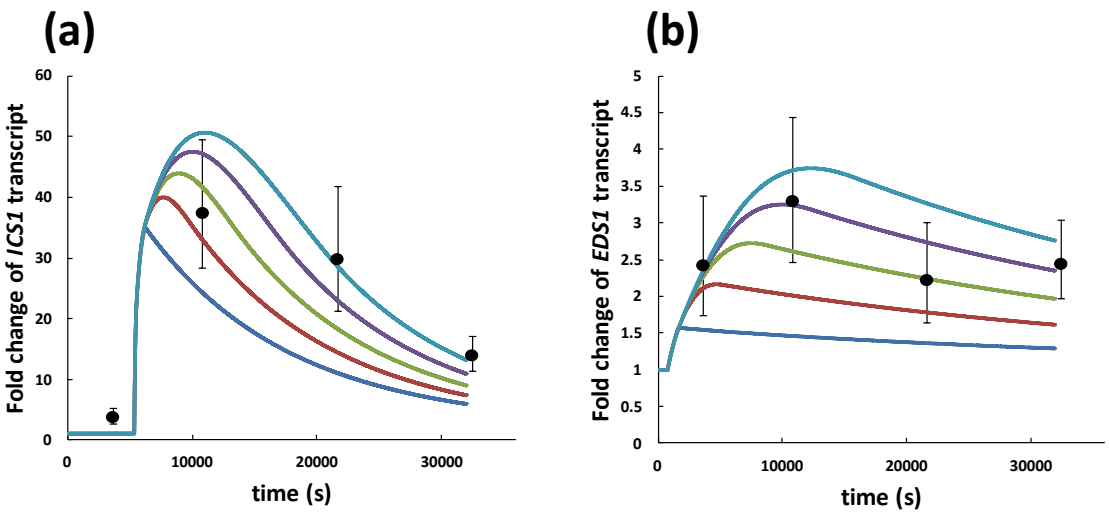
(a)
Fold change of ICS1 transcript
60
50
40
30
20
10
0
0
10000
20000
30000
time (s)
(b)
Fold change of EDS1 transcript
5
4.5
4
3.5
3
2.5
2
1.5
1
0.5
0
0
10000
20000
30000
time (s)

FIGURE 5

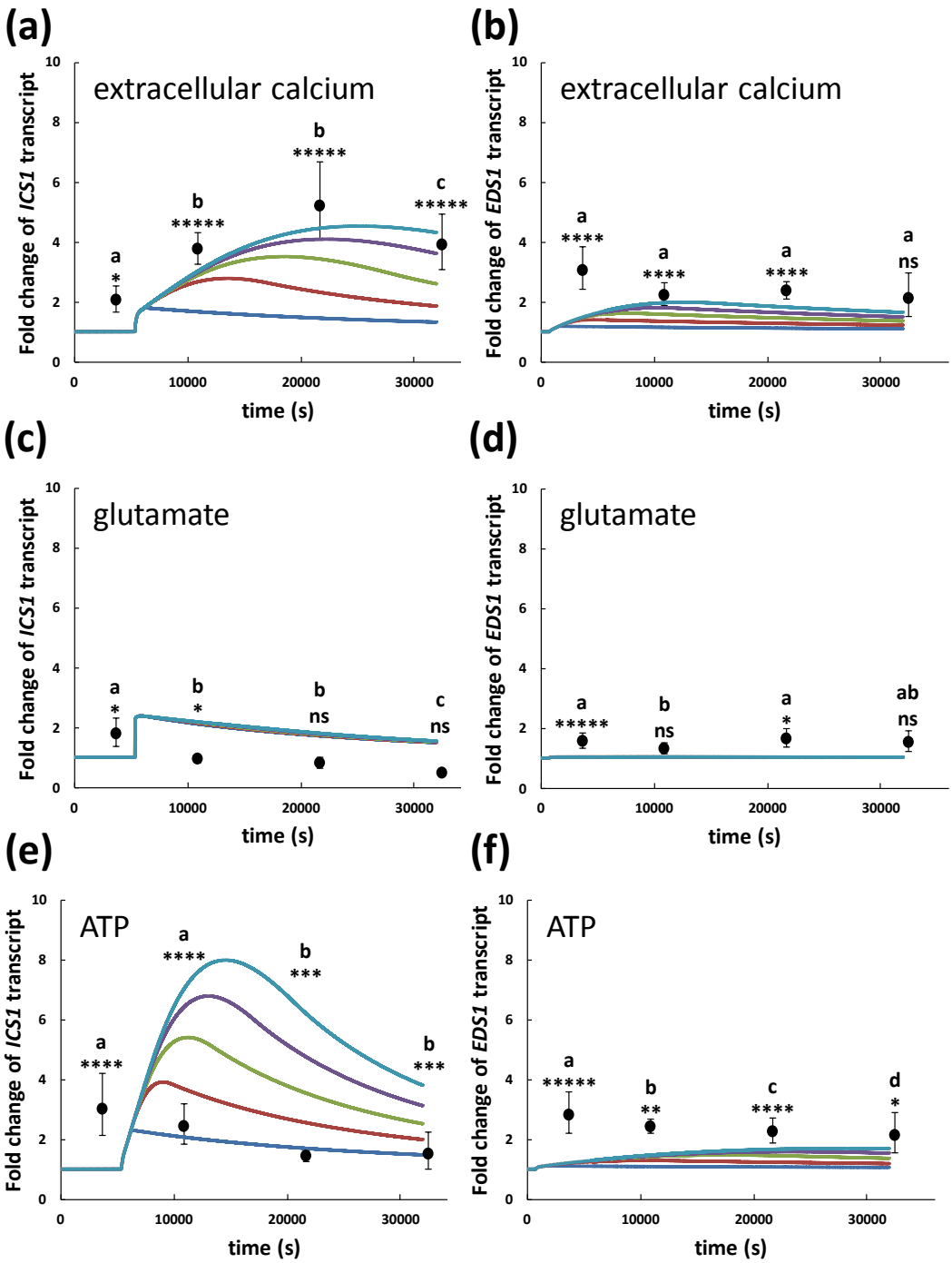
(a)
extracellular calcium
Fold change of ICS1 transcript
time (s)
a
*
b
*****
b
*****
c
*****
(b)
extracellular calcium
Fold change of EDS1 transcript
time (s)
a
****
a
****
a
****
a
ns
(c)
glutamate
Fold change of ICS1 transcript
time (s)
a
*
b
*
b
ns
c
ns
(d)
glutamate
Fold change of EDS1 transcript
time (s)
a
*****
b
ns
a
*
ab
ns
(e)
ATP
Fold change of ICS1 transcript
time (s)
a
****
a
****
b
***
b
***
(f)
ATP
Fold change of EDS1 transcript
time (s)
a
*****
b
**
c
****
d
*

FIGURE 6